The Combined Antitumor Effects of [125]I Radioactive Particle Implantation and Cytokine-Induced Killer Cell Therapy on Xenograft Hepatocellular Carcinoma in a Mouse Model

Junyong Zhang, PhD[1,2], Nian Wu, MM[3], Zhengrong Lian, PhD[4],
Huyi Feng, PhD, MD[3], Qing Jiang, PhD, MD[2], Xianfeng Chen, MM[5],
Jianping Gong, PhD, MD[1], and Zhengrong Qiao, PhD[6]

Abstract

The combination of radiotherapy and immunotherapy has shown great promise in eradicating tumors. For example, ^{125}I radioactive particle implantation and cytokine-induced killer cell therapies have demonstrated efficacy in treating hepatocellular carcinoma. However, the mechanism of this combination therapy remains unknown. In this study, we utilized cytokine-induced killer cells obtained from human peripheral blood mononuclear cells along with ^{125}I radioactive particle implantation to treat subcutaneous hepatocellular carcinoma xenograft tumors in BALB/c nude mice. The effects of combination therapy on tumor growth, tumor cell apoptosis and proliferation, animal survival, and immune indexes were then assessed. The results indicated that ^{125}I radioactive particle implantation combined with cytokine-induced killer cells shows a much greater antitumor therapeutic effect than either of the therapies alone when compared to control treatments. Mice treated with a combination of radiotherapy and immunotherapy displayed significantly reduced tumor growth. [125]I radioactive particle implantation upregulated the expression of major histocompatibility complex (MHC) class I chain-related gene A in hepatocellular carcinoma cells and enhanced cytokine-induced killer cell–mediated apoptosis through activation of caspase-3. Furthermore, cytokine-induced killer cells supplied immune substrates to induce a strong immune response after ^{125}I radioactive particle implantation therapy. In conclusion, ^{125}I radioactive particle implantation combined with cytokine-induced killer cell therapy significantly inhibits the growth of human hepatocellular carcinoma cells in vivo and improves animal survival times through mutual promotion of antitumor immunity, presenting a promising therapy for hepatocellular carcinoma.

[1] Chongqing Key Laboratory of Hepatobiliary Surgery, Department of Hepatobiliary Surgery, the Second Affiliated Hospital of Chongqing Medical University, Chongqing, People's Republic of China
[2] Department of Urology Surgery, the Second Affiliated Hospital of Chongqing Medical University, Chongqing, People's Republic of China
[3] Department of General Surgery, the Fifth People's Hospital of Chongqing City, Chongqing, People's Republic of China
[4] Department of Clinical Epidemiology and Biostatistics, Population Health Research Institution, McMaster University, Hamilton, Ontario, Canada
[5] Department of Hepatobiliary Surgery, Fuling Center Hospital, Fuling District, Chongqing, People's Republic of China
[6] Department of General Surgery, People's Hospital of Changshou District, Chongqing, People's Republic of China

Corresponding Authors:
Qing Jiang, PhD, MD, Department of Urology Surgery, the Second Affiliated Hospital of Chongqing Medical University, Chongqing, People's Republic of China.
Email: jq001002@sina.com

Jianping Gong, PhD, MD, Chongqing Key Laboratory of Hepatobiliary Surgery, Department of Hepatobiliary Surgery, the Second Affiliated Hospital of Chongqing Medical University, No 76, Linjiang road, Yuzhong District, Chongqing, 400010, People's Republic of China.
Email: gjp_cqmu@yeah.net

Zhengrong Qiao, PhD, Department of General Surgery, People's Hospital of Changshou District, No 16, Northern of Fengcheng Street, Changshou District, Chongqing 401220, People's Republic of China.
Email: 471885922@qq.com

Introduction

Hepatocellular carcinoma (HCC) ranks as the sixth most common malignant cancer and is the second leading cause of cancer-related death worldwide. China accounts for about 50% of the total number of both HCC cases and HCC-related deaths.[1] In China, patients with HCC often have hepatitis B or cirrhosis and are frequently diagnosed at later stages when radical surgery is no longer an effective treatment.[2] To qualify for radical surgery, patients with HCC must have sufficient liver function, which is preserved in only 30% to 40% of cases.[2] Furthermore, frequent recurrence of HCC also limits clinical effectiveness of surgical treatment strategies. For patients with recurrent or advanced stage HCC, radiotherapy and chemotherapy are the primary treatment options.[3] However, patients with HCC undergoing radiotherapy often have serious adverse effects and experience high tumor recurrence rates.[4] Thus, radiotherapy has been previously excluded in many liver cancer treatment guidelines based on cost–benefit analysis.[5]

Currently, the radiosensitivity of HCC cells is considered to be comparable to poorly differentiated squamous cell carcinoma. [125]I radioactive particle implantation (RPI) is an effective therapy for advanced HCC due to its controllable and continuous γ and X-ray radiation range and mild adverse effects.[6,7] Additionally, studies have demonstrated that local radiotherapy enhances the tumor-specific immune response.[8,9] Patients with advanced HCC usually experience decreased immune cell numbers and function, which hampers the effects of local radiotherapy on antitumor immunity. Thus, one method for enhancing the efficacy of radioactive ^{125}I RPI to treat advanced HCC may be through the addition of cell therapy treatment with antitumor immune cells.

Cytokine-induced killer (CIK) cell therapy complements ^{125}I RPI therapy by addressing the lack of immune cells that are poised to provide antitumor immunity. Cytokine-induced killer cells are CD3 and CD56 double-positive T cells that are differentiated from peripheral blood mononuclear cells (PBMCs) after *in vitro* stimulation with a variety of cytokines.[10] Cytokine-induced killer cells possess powerful restricted tumoricidal effects (RTEs), similar to T cells, and a non-RTE (NRTE), similar to natural killer cells. Consequently, CIK cells are considered to be antitumor immunocytes with powerful antitumor effects and a wide spectrum of antitumor activities. Cytokine-induced killer cell therapy has the potential to radically improve the treatment of small residual tumors and improve antitumor immunocompetence with both its RTE and NRTE.[11-16]

Based on previous studies, we hypothesized that CIK cell therapy could improve the antitumor immune response and enhance the curative effect of ^{125}I RPI by supplying a population of primed antitumor immunocytes. Furthermore, ^{125}I RPI could expose the major histocompatibility complex (MHC) class I polypeptide-related sequence A (MICA) of HCC cells to CIK cells, which in turn would result in tumor cell apoptosis. In this study, a total of 65 nude mice were treated with CIK cell therapy, radioactive ^{125}I particle implantation, or both. Tumor growth and survival rates were analyzed over time, and mechanisms of this combination therapy were explored.

Materials and Methods

Animal Model Establishment

We chose the SMMC-7721[17] human HCC cell line for its ease of culture and effective tumorigenic ability. The SMMC-7721 cell line we used was acquired from Life Sciences Institute of Chongqing Medical University with previous verification of identity. The cells were cultured in Dulbecco's modified eagle medium (high glucose; Hyclone, Massachusetts, USA) with 10% fetal bovine serum (FBS; Hyclone) and 1% penicillin and streptomycin (Boster, Wuhan, China) at 37°C with 5% CO_2. Animal experiments were approved by the ethics committee of Chongqing Medical University. Sixty-five healthy, 4-week-old male BALB/c nude mice were purchased from the Institute for Laboratory Animal Research, Peking Union Medical College. To establish an HCC animal model, 200 to 300 μL SMMC-7721 cell suspension, containing 3×10^5 to 3×10^6 cells, was injected subcutaneously into the right flank of BALB/c nude mice. Apparent HCC tumors of 0.5 to 0.6 cm in diameter were observed after 14 days. After xenografts were established (14 days), mice were randomly divided into various treatment

groups including the ^{125}I RPI group (n = 16), the CIK cell group (n = 16), the combination therapy group (n = 17), and the untreated control group (n = 16).

Isolation of PBMCs

Procedures for peripheral blood collection from human donors and PBMC isolation were approved by the ethics committee of Chongqing Medical University. All donors were aware of this experiment and provided written informed consent. Thirty milliliter of peripheral blood from each healthy donor was collected into tubes containing heparin and mixed with isopycnic phosphate-buffered saline (PBS). The aforementioned mixture placed in a centrifuge tube and spread on the surface of 4 mL human peripheral blood lymphocyte separation medium (Haoyang Company, Shanghai, China) to form a clear boundary. Tubes were centrifuged at 2000 rpm for 20 minutes at room temperature. The thin gray white layer of mononuclear cells between the first layer of blood plasma and the second layer of separation medium was drawn into the tubes with 4 mL PBS and centrifuged at 1500 rpm for 10 minutes at room temperature to remove platelets. Trypan blue used to ensure viability was greater than 95%.

Cytokine-Induced Killer Cell Collection and Therapy

Cytokine-induced killer cells were collected as described previously by Franceschetti et al.[18] Peripheral blood mononuclear cells were washed with PBS and cultured in Roswell Park Memorial Institute 1640 (Hyclone) medium with a 10% FBS and 1% penicillin–streptomycin combination at a cell density of 1×10^{6}/mL. Cultures were supplemented with human interferon γ (IFN-γ) at a final concentration of 1000 U/mL. After 24 hours, human anti-CD3 antibody (50 ng/mL) and interleukin 2 (IL-2; 500 U/mL) were added to promote maturation of CIK cells. Interleukin 2 (500 U/mL) was added every 3 days with the exchange of cell medium, and cells were cultured for 15 days. The CIK phenotype was verified by flow cytometry with CD3 and CD56 double-positive staining, and the double-positive rate attained was 20%. For treatment, 3×10^{7} CIK cells were injected via caudal veins of HCC xenograft mice 4 times a week, beginning on the next day (which is labeled as 0th day in Figure 1A) after the establishment of the animal model.

[125]I RPI Therapy

[125]I RPI therapy began on the next day (which is labeled as 0th day in Figure 1A) after the establishment of the animal model. Radioactive ^{125}I particles (18.5 MBq [0.5 mCi], 180 days of validity; ZhiBo Bio-Medical Technology Company, Shanghai, China) were prepared in a #18 puncture needle. Tumors were punctured at the points where 0.5 cm away from the center of the tumor, where the depth of needle insertion was estimated and marked. The needle was inserted horizontally and the needle core containing the ^{125}I particles was inserted into the center of the tumor. After implantation was completed, the needle

and needle core were fixed and extracted. The puncture point on the animal model was compressed and disinfected. The animals were observed for 10 minutes after ^{125}I particle implantation and then their activity and diet were observed, noted, and evaluated the following day.

Xenograft Growth Analysis of Animal Models

The animal model was successfully established 14 days after the initial subcutaneous injection of SMMC-7721 cell suspension. At that point, tumor volumes were measured and recorded every 4 days and calculated as $ab2/2$ (a = the long diameter, b = the short diameter). Tumor growth curves were drawn according to these values. Tumor inhibitory rate (TIR) was calculated as $(D - X)/D \times 100\%$ (D represents the average tumor volume in the control group, X represents the average tumor volume in treatment groups) after 32 days of therapy.

Immunohistochemical and Western Blot Assays

After 32 days of therapy, 5 nude mice in every group were killed for collection of tumor samples and blood samples (used for enzyme linked immunosorbent assay [ELISA], described later). Samples were processed and placed on microscope slides that were used for hematoxylin and eosin (H&E) staining, terminal deoxynucleotidyl transferase (TdT)-mediated dUTP nick end labeling (TUNEL) assay (DeadEnd Colorimetirc TUNEL system, Sigma, Darmstadt, Germany), and immunohistochemical (IHC) assay for Ki-67 protein (with polyclonal antibody of Ki-67; Zhongshan Golden Bridge, Beijing, China). Three slices from each nude mouse were analyzed by Image Pro-plus 6.0 software, and 3 random visual fields were selected to quantify the optical density (OD) value of targeted molecules. The rest of the tumor tissue samples was placed in liquid nitrogen and total proteins were used for Western blots to detect MICA and caspase-3 expression (with polyclonal antibody of β-actin [Zhongshan Golden Bridge] and polyclonal antibody of MICA and polyclonal antibody of caspase-3 [Abcam, United Kingdom]).

Enzyme-Linked Immunosorbent Assays to Measure Cytokine Levels

Blood samples were collected into centrifuge tubes with thromboplastic medicaments and then stood at room temperature until the blood coagulated. Samples were then centrifuged at 3000 rpm for 10 minutes, and the supernatant was drawn for testing. Enzyme-linked immunosorbent assays for serum IL-2, IL-6, tumor necrosis factor α (TNF-α), and IFN-γ were performed according to manuals of the ELISA kits (Cusabio, Baltimore, USA).

Statistical Analysis

Kaplan-Meier method was used to generate the survival curve of the remainder of the nude mice (^{125}I RPI group [n = 11], the
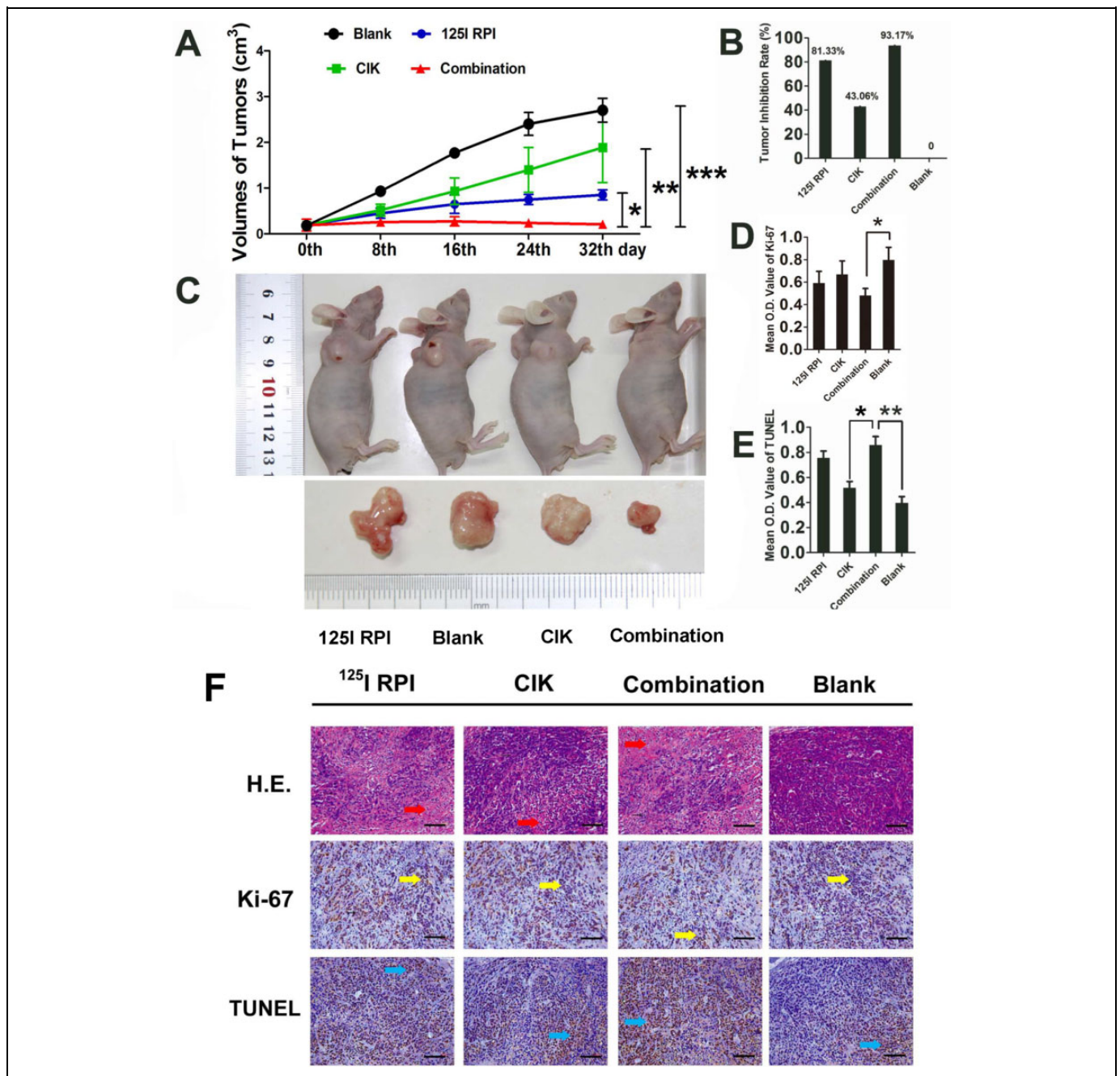
Figure 1. Therapeutic effects of ^{125}I RPI or/and CIK cells to HCC xenografts in BALB/c nude mice. A, B, and C, Thirty-two days after the initiation of treatment, the tumor volumes in the ^{125}I RPI group and the CIK cell group were significantly smaller than those in control groups. The smallest tumor sizes were observed in the combination therapy group when compared to other groups ($*P < .05$, $**P < .01$, $***P < .001$). The highest TIR was observed in the combination therapy group. D, E, and F, The images were taken randomly, not intentionally. Statistically significant differences were observed in the mean OD values of Ki-67 and TUNEL staining between the control group and treatment groups. The combination of ^{125}I particle implantation and CIK cell therapy showed the highest inhibition of tumor cell proliferation and induction of apoptosis ($*P < .001$, $F = 318.373$; $***P < .001$, $F = 24.334$, respectively). The only significant differences in TUNEL OD values between treatment groups were observed between the CIK cell therapy group and the combination therapy group ($**P < .001$, $F = 207.491$). CIK indicates cytokine-induced killer; HCC, hepatocellular carcinoma; OD, optical density; RPI, radioactive particle implantation; TIR, tumor inhibitory rate; TUNEL, terminal deoxynucleotidyl transferase(TdT)-mediated dUTP nick end labeling.

CIK cell group [n = 11], the combination therapy group [n = 12], and the untreated control group [n = 11]). The data were analyzed with log-rank test.

The data were analyzed using the Statistical Package for the Social Sciences 18.0 (SPSS, Inc, Chicago, Illinois), with $P < .05$ taken as statistically significant. Data are represented as mean
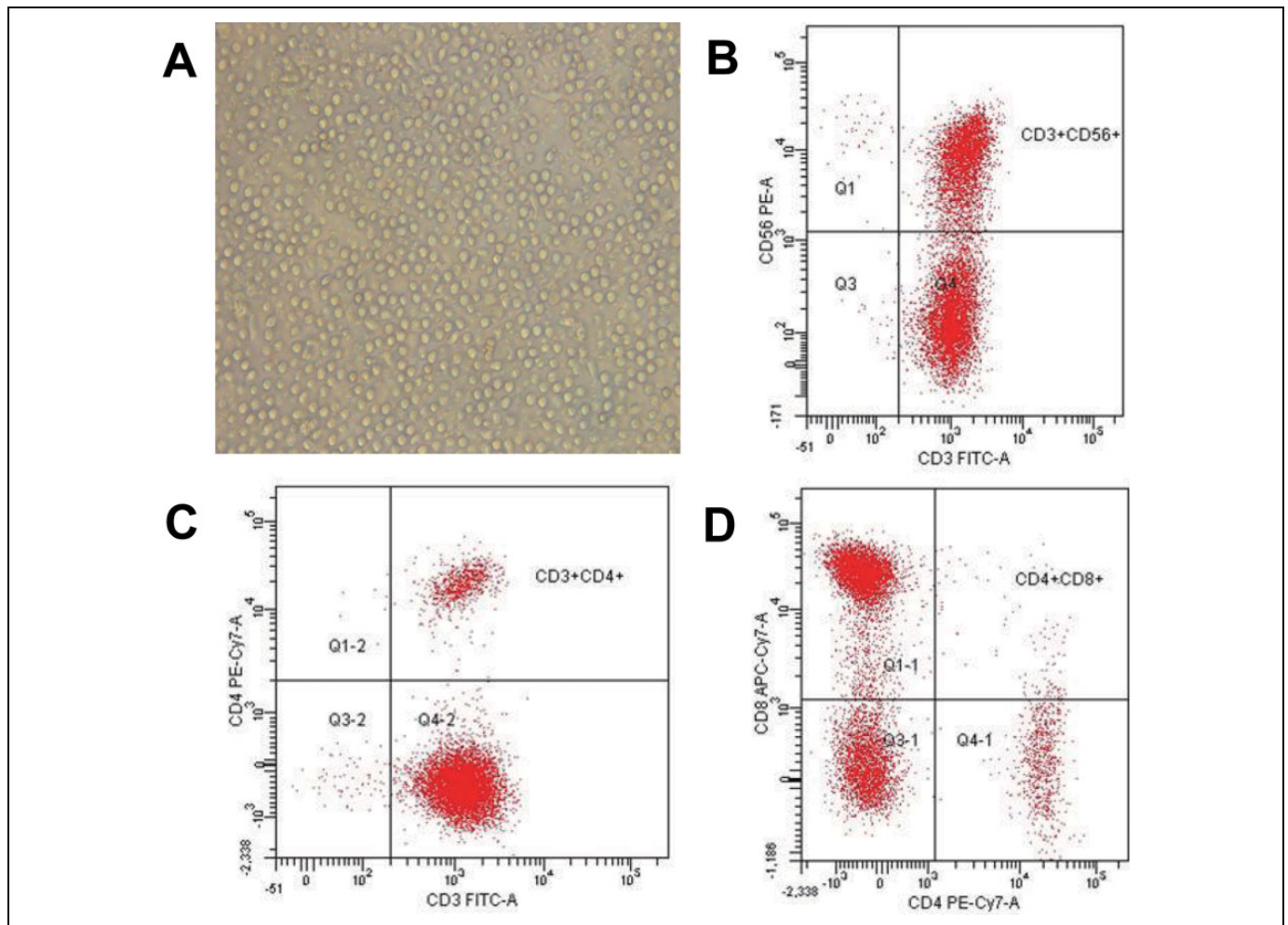
Figure 2. Isolation and identification of CIK cells. Cytokine-induced killer cells were isolated from human PBMCs, cultured in media supplemented with differentiation factors, and then observed under a light microscope. A, Cytokine-induced killer cells demonstrated sufficient cell numbers (×200). Cytokine-induced killer cells were identified by flow cytometry with CD3 and CD56 double-positive staining at a rate of 42.5% (11.7%). CIK indicates cytokine-induced killer; PBMC, peripheral blood mononuclear cells.

(standard deviation [SD]) of at least 3 independent experiments. Repeated-measures analysis of variance (ANOVA) was used for comparison within each group. One-way ANOVA was used for comparison between each group. The LSD (Least-Significant difference)-t method was applied for multiple comparisons.

Results

Collection and Identification of CIK Cells

After stimulation of human PBMCs with IFN-γ, anti-CD3 antibody, and IL-2 for 15 days, analysis of CIK cell markers was performed. Flow cytometry assays demonstrated that CD3 and CD56 double-positive rates of these cells were 42.5% (11.7%) (89.9% [21.5%] CD3$^+$, 61.4% [13.8%] CD3$^-$CD56$^+$, 42.5% [11.7%] CD3$^+$CD56$^+$, 0.7% [0.23%] CD3$^+$CD56$^-$, 56.1% [19.4%] CD8$^+$CD4$^-$, 7.9% [0.9%] CD4$^+$CD8$^-$; Figure 2). These results verify the successful differentiation of CIK cells from human PBMCs.

Combination of Radiotherapy and CIK Cell Therapy Significantly Suppressed In Vivo HCC Growth

Tumor volumes in the ^{125}I RPI group, the CIK cell group, and the combination therapy group showed significantly slower growth when compared with the control group. After 32 days of treatment, significantly smaller tumors were observed in both the ^{125}I RPI group and the CIK cell group (TIRs were 81.33% and 43.06%, respectively). The greatest reduction in tumor growth was observed in the combination therapy group, in which tumors stopped growing and appeared to shrink (TIR was 93.17%), indicating that combination of ^{125}I RPI and CIK cell therapy resulted in strong antitumor effects that exceeded single therapy of either ^{125}I RPI or CIK cell therapy (Figures 1A-C). In addition, tumor volumes in the ^{125}I RPI group were smaller than those in the CIK cell group, indicating that ^{125}I RPI could induce more powerful destruction of tumor cells by direct γ radiation.
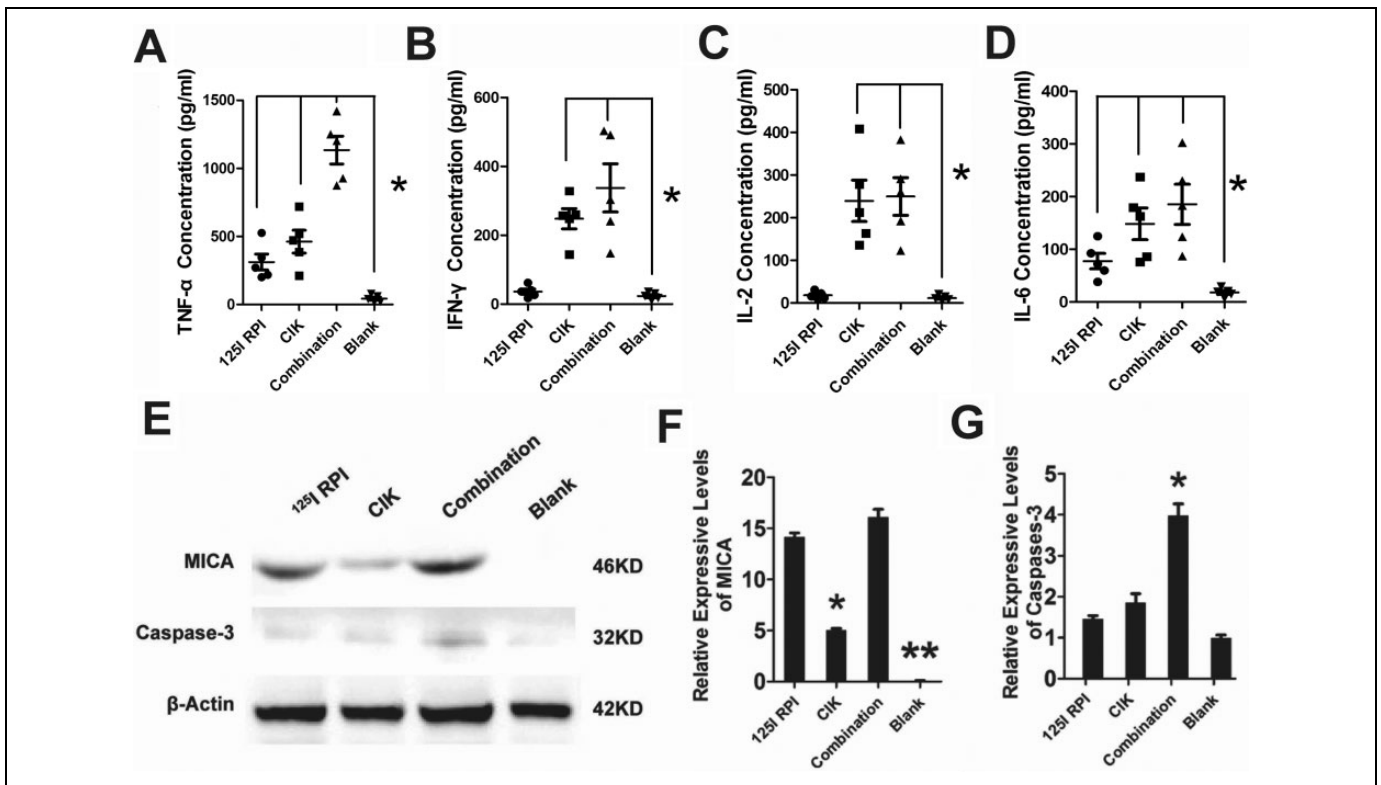
Figure 3. The antitumor mechanism associated with combination of ^{125}I RPI and CIK cell therapy. A, B, C, and D, Levels of various inflammatory markers in the serum of HCC xenograft mice with or without treatment were assessed by ELISA. Compared to the control group, ^{125}I RPI induced significant increases in only TNF-α and IL-6 plasma levels, whereas CIK cell therapy led to an increase in all inflammatory molecules tested. Combination treatment with ^{125}I RPI and CIK cell therapy induced the highest levels of TNF-α, IFN-γ, IL-2, and IL-6 in serum of nude mice (*$P < .05$). E, F, and G, The MICA expression downregulation was observed in untreated tumors. After either ^{125}I RPI therapy, CIK cell therapy, or combined therapy, MICA expression by tumor cells was significantly upregulated (**$P < .01$, compared to the control group). Among the 3 therapy groups, the MICA protein levels in tumors increased the least in the CIK cell therapy group (*$P < .05$, compared to the ^{125}I RPI group and the combination therapy group). The highest caspase-3 protein level was observed in the combination group (*$P < .05$, compared to other groups), but no statistically significance differences of caspase-3 level were seen between the other 3 groups. CIK indicates cytokine-induced killer; ELISA, enzyme-linked immunosorbent assay; HCC, hepatocellular carcinoma; IFN-γ, interferon γ; IL, interleukin; MICA, MHC, major histocompatibility complex; class I polypeptide-related sequence A; RPI, radioactive particle implantation; TNF-α, tumor necrosis factor alpha.

The Combination of Radiotherapy and CIK Cell Therapy Significantly Inhibited HCC Cell Proliferation and Promoted Apoptosis

Varying degrees of tumor cell necrosis and apoptosis were observed by H&E staining in all groups that received treatments. Significant necrosis was found in the ^{125}I RPI group and the combination therapy group (Figure 1F, indicated by red arrows) but not in the CIK cell therapy–only group. Ki-67 levels in tumor tissue were significantly reduced by ^{125}I RPI, CIK therapy, and the combination treatment (Figure 1F, indicated by yellow arrows), indicating that all 3 treatment groups decreased tumor cell proliferation. The TUNEL assays indicated marked apoptosis of tumor cells upon treatment (Figure 1F, indicated by blue arrows). Compared to the control group, the combination therapy showed significant inhibition of tumor cell proliferation ($P < .05$; Figure 1D) and induction of apoptosis ($P < .001$; Figure 1E). No significant differences

were observed when comparing Ki-67 protein levels between the ^{125}I RPI group and the combination therapy group or between the CIK cell group and the combination therapy group, although the levels in the combination therapy group tended to be lower. A significant increase in the TUNEL mean OD could be found in the combination group when compared with that in the CIK cell group ($P < .001$). No statistical difference in TUNEL mean OD values could be observed between the ^{125}I RPI group and the combination therapy group ($P > .05$).

Enzyme-Linked Immunosorbent Assays Reveal Reciprocal Promotion of Antitumor Immune Responses Induced by Combination of Radiotherapy and CIK Cell Therapy

Due to the damage of tumor tissue by radiation from ^{125}I RPI, damage-associated products from tumors stimulated

nonspecific immunity and inflammatory molecules such as TNF-α and IL-6, which were significantly increased compared to the control group (Figure 3A and D). However, IFN-γ and IL-2 did not increase after radiation from ^{125}I RPI, which is likely due to the absence of T cells in nude mice (Figure 3B and C). All TNF-α, IFN-γ, IL-2, and IL-6 levels in serum of nude mice in the CIK cell group were higher than those in the ^{125}I RPI group, indicating that the CIK cells induced a strong anti-tumor immune response. The highest levels of TNF-α, IFN-γ, IL-2, and IL-6 were observed in the ^{125}I RPI and CIK combination group, indicating an additive enhancement of the anti-tumor immune response by CIK cell therapy and ^{125}I RPI.

[125]I RPI Upregulated MICA Expression Enhanced Caspase-3-Induced HCC Cells Apoptosis by CIK Cells

The MICA expression was barely detectable in untreated tumors. In contrast, ^{125}I RPI, CIK cell treatment, and combination therapy all significantly upregulated MICA expression xenograft HCC tumors compared to the control group (Figure 3E and F; $P < .01$). Although MICA was expressed in CIK cell therapy groups, it was at much lower levels than the treatments that included ^{125}I RPI (Figure 3F, compared to the ^{125}I RPI group and the combination therapy group; $P < .05$). No significant difference in MICA expression was observed between the ^{125}I RPI group and the combination therapy group (Figure 3F; $P > .05$). Significantly higher caspase-3 protein levels were observed only in the combination therapy group (Figure 3E and G; $P < .05$), indicating the highest levels of apoptosis were present in the combination therapy group.

The Combination Therapy Distinctly Improved Survival of Model Animals

Survival curves of the remaining nude mice (11 mice in each of the ^{125}I RPI, CIK cells, and blank groups and 12 mice in the combination group) were analyzed using the Kaplan-Meier method (Figure 4). Significantly better survival was observed in mice with combination therapy when compared to the ^{125}I RPI group ($P = .001$, log-rank method), the CIK cell group ($P < .001$), and the blank group ($P < .001$). Both the CIK cell therapy and ^{125}I RPI groups showed significant improvement in survival when compared to the control group ($P = .007$ in the ^{125}I RPI group and .007 in the CIK cell group). However, there was no statistical difference in survival between the CIK cell and ^{125}I RPI groups ($P = .849$). These results indicate that the ^{125}I radioactive particles along with CIK cell therapy could significantly improve the prognosis of nude mice with subcutaneously transplanted HCC tumors.

Discussion

The clinical efficacy of ^{125}I RPI for the treatment of HCC has been previously demonstrated.[7,19-21] The effectiveness of ^{125}I particle RPI treatment is due to direct cytotoxic effects of radiation on tumor cells along with the stimulation of tumor-
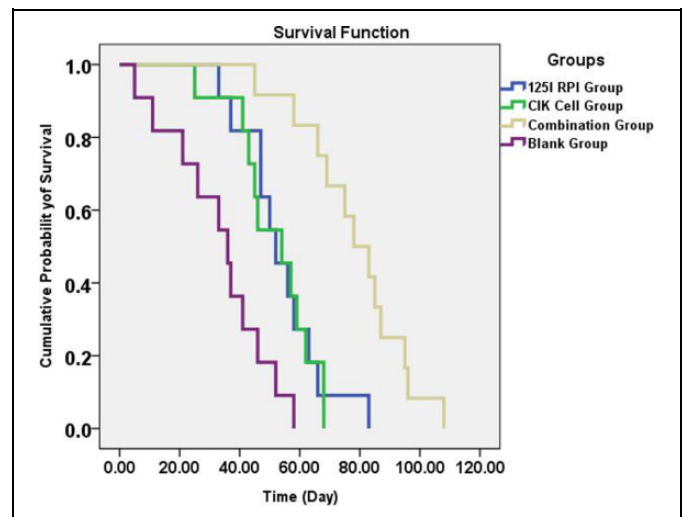

Figure 4. Survival analysis of HCC xenograft BALB/c mice treated or not with ^{125}I RPI and CIK cell therapy alone or in combination. Survival curves of BALB/c nude mice treated with the indicated therapies are depicted following the Kaplan-Meier method. Nude mice in the combination therapy group showed significantly better survival when compared to all other groups ($P < .05$). Both the ^{125}I RPI group ($P = .007$) and CIK cell group ($P = .007$) showed better survival than the control group; however, no statistically significant difference in survival comparison could be found between the 2 individual therapies ($P = .849$). CIK indicates cytokine-induced killer; HCC, hepatocellular carcinoma; RPI, radioactive particle implantation.

specific immune response and innate immunity by radiation.[8,9] Unfortunately, patients with advanced HCC are often immunocompromised and display decreased immune cell abundances and activity. Without an adequate immune system, the apoptotic products released by tumor cells after ^{125}I RPI therapy may not induce a sufficient tumor-specific immune response, thereby limiting the therapeutic effects of ^{125}I particle implantation.

Cytokine-induced killer cell therapy compensates for the deficient immune response observed with ^{125}I RPI therapy in advanced HCC by inducing direct tumor cytotoxicity along with mediating innate immunity and tumor-specific immune responses after the destruction of tumor cells by radiation. Numerous reports have demonstrated that the use of adjuvant CIK cell therapy may significantly improve the prognosis of patients with malignant tumors, including HCC.[9,22-24] Mechanisms by which CIK cells destroy tumors include the induction of tumor cell apoptosis directly through expression of the Fas ligand protein.[25] Additionally, a large number of antitumor cytokines are released from activated CIK cells, such as IFN-γ, IL-2, IL-6, and TNF-α, which inhibit tumor growth, enhance antitumor immunity,[26] and activate apoptotic genes such as Bcl-2 (B-cell lymphoma-2), Bcl-xL (B-cell lymphoma-XL), DAD1 (defender against cell death 1).[27] Finally, CIK cells express 2 surface molecules, NKG2D (natural-killer group 2, member D) and DAP10 (DNAX-activation protein 10), which are involved in antitumor immunity. NKG2D binds to MIC-A/B (Major histocompatibility complex class I-related chain A/B)

and the UL16 (unique long 16 protein) mucoprotein family (ULPBs 1, 2, 3) that are highly expressed on the surface of tumor cells. After binding to these molecules on the tumor cell, perforin, glycoprotein, lysosomal enzyme, and granzyme are released from CIK cells and induce lysis of tumor cells.[13,28] DAP10 enhances the NKG2D pathway.[29] However, reports have demonstrated that MICA is not frequently expressed by HCC cells.[30,31] Therefore, upregulating MICA on HCC cells, which is observed with ^{125}I RPI treatment, may be an effective strategy to increase the antitumor effects of CIK cells.

BALB/c nude mice with cellular immunodeficiency were used as animal models in this study to simulate the immunodeficiency observed in patients with advanced HCC. Although the use of ^{125}I RPI or CIK cell therapy alone was able to induce apoptosis and inhibit the proliferation of subcutaneous xenografts, as shown through IHC, dual ^{125}I RPI and CIK cell therapy led to a significantly greater antitumor effect. Due to the destruction of tumor tissue by ^{125}I RPI and the limited field of vision allowed by light microscopes, no obvious superposition effects on proliferation and apoptosis were observed in the combination therapy group. However, a significantly wider range of proliferation inhibition and apoptosis induction was observed in the combination of ^{125}I RPI and CIK cell therapy groups.

We also investigated whether the antitumor effects of these therapies was independent or mutually beneficial. The expression levels of MICA and caspase-3 were assessed through Western blots and expression of immunomodulatory factors, such as TNF-α, IFN-γ, IL-2, and IL-6, was assessed through ELISAs. A significant increase in MICA expression was observed in HCC cells treated with ^{125}I RPI, which may have been responsible for the increased MICA-NKG2D-induced antitumor effect of CIK cells. Evidence of this enhancement was provided by the increased caspase-3 levels observed in the combination therapy group compared to individual treatments. Due to thymus and T-cell deficiencies, BALB/c nude mice could not mount a sufficient cellular immune response when exposed to the products of apoptotic and necrotic tumor cells induced by radiation. Consequently, all immune indexes in the ^{125}I particle implantation group increased, except IL-2 and IFN-γ. Meanwhile, all immune indexes, including the IL-2 and IFN-γ, were increased in the CIK cell treatment group. Furthermore, CIK cell therapy enhanced the antitumor immune response following ^{125}I RPI therapy, which was also associated with the highest levels of TNF-α, IFN-γ, IL-2, and IL-6. Therefore, the antitumor effects of the combination of 125-RPI and CIK cell therapy were synergistic rather than additive, indicating a mutually beneficial reaction between the 2 therapies.

Conclusion

Radiation from ^{125}I RPI exposed MICA expression on HCC cells, which in turn enhanced NKG2D-MICA-induced lysis of tumor cells by CIK cells.[32,33] Meanwhile, CIK cells provided immune cells and immune factors for patients with immunodeficient HCC who underwent ^{125}I RPI therapy and supplied immune substrates for radiotherapy-related immunoreaction. Thus, the combination of ^{125}I RPI and CIK cell therapy could become a promising therapeutic strategy for patients with advanced HCC.

References

1. Torre LA, Bray F, Siegel RL, Ferlay J, Lortet-Tieulent J, Jemal A. Global cancer statistics, 2012. *CA Cancer J Clin*. 2015;65(2): 87-108.

2. Li C, Wen TF, Yan LN, et al. Scoring selection criteria including total tumour volume and pretransplant percentage of lymphocytes to predict recurrence of hepatocellular carcinoma after liver transplantation. *PLoS One*. 2013;8(8):e72235.

3. Fujino H, Kimura T, Aikata H, et al. Role of 3-D conformal radiotherapy for major portal vein tumor thrombosis combined with hepatic arterial infusion chemotherapy for advanced hepatocellular carcinoma. *Hepatol Res*. 2015;45(6):607-617.

4. Tao C, Yang LX. Improved radiotherapy for primary and secondary liver cancer: stereotactic body radiation therapy. *Anticancer Res*. 2012;32(2):649-655.

5. Wu ZF, Zhou XH, Hu YW, et al. TLR4-dependant immune response, but not hepatitis B virus reactivation, is important in radiation-induced liver disease of liver cancer radiotherapy. *Cancer Immunol Immunother*. 2014;63(3):235-245.

6. Chen K, Chen G, Wang H, et al. Increased survival in hepatocellular carcinoma with iodine-125 implantation plus radiofrequency ablation: a prospective randomized controlled trial. *J Hepatol*. 2014;61(6):1304-1311.

7. Peng S, Yang QX, Zhang T, et al. Lobaplatin-TACE combined with radioactive ^{125}I seed implantation for treatment of primary hepatocellular carcinoma. *Asian Pac J Cancer Prev*. 2014;15(13): 5155-5160.

8. Sebastian M, Papachristofilou A, Weiss C, et al. Phase Ib study evaluating a self-adjuvanted mRNA cancer vaccine (RNActive) combined with local radiation as consolidation and maintenance treatment for patients with stage IV non-small cell lung cancer. *BMC Cancer*. 2014;14:748.

9. Ma Y, Xu YC, Tang L, Zhang Z, Wang J, Wang HX. Cytokine-induced killer (CIK) cell therapy for patients with

hepatocellular carcinoma: efficacy and safety. *Exp Hematol Oncol*. 2012;1(1):11.

10. Hiniker SM, Chen DS, Reddy S, et al. A systemic complete response of metastatic melanoma to local radiation and immunotherapy. *Transl Oncol*. 2012;5(6):404-407.

11. Schmidt-Wolf IG, Negrin RS, Kiem HP, Blume KG, Weissman IL. Use of a SCID mouse/human lymphoma model to evaluate cytokine-induced killer cells with potent antitumor cell activity. *J Exp Med*. 1991;174(1):139-149.

12. Thanendrarajan S, Kim Y, Schmidt-Wolf IG. New adoptive immunotherapy strategies for solid tumors with CIK cells. *Expert Opin Biol Ther*. 2012;12(5):565-572.

13. Schmeel LC, Schmeel FC, Coch C, Schmidt-Wolf IG. Cytokine-induced killer (CIK) cells in cancer immunotherapy: report of the international registry on CIK cells (IRCC). *J Cancer Res Clin Oncol*. 2015;141(5):839-849.

14. Schlimper C, Hombach AA, Abken H, Schmidt-Wolf IG. Improved activation toward primary colorectal cancer by antigen-specific targeting autologous cytokine-induced killer cells. *Clin Dev Immunol*. 2012;2012:238924.

15. Hu H, Qiu Y, Guo M, et al. Targeted Hsp70 expression combined with CIK-activated immune reconstruction synergistically exerts antitumor efficacy in patient-derived hepatocellular carcinoma xenograft mouse models. *Oncotarget*. 2015;6(2): 1079-1089.

16. Jiang J, Wu C, LU B. Cytokine-induced killer cells promote antitumor immunity. *J Transl Med*. 2013;11:83.

17. Liu Y, Bi T, Dai W, et al. Effects of oxymatrine on the proliferation and apoptosis of human hepatoma carcinoma cells. *Technol Cancer Res Treat*. 2016;15(3):487-497.

18. Franceschetti M, Pievani A, Borleri G, et al. Cytokine-induced killer cells are terminally differentiated activated CD8 cytotoxic T-EMRA lymphocytes. *Exp Hematol*. 2009;37(5): 616-628.

19. Kollmeier MA, Pei X, Algur E, et al. A comparison of the impact of isotope [(125)I vs. (103)Pd] on toxicity and biochemical outcome after interstitial brachytherapy and external beam radiation therapy for clinically localized prostate cancer. *Brachytherapy*. 2012;11(4):271-276.

20. Yang M, Fang Z, Yan Z, et al. Transarterial chemoembolisation (TACE) combined with endovascular implantation of an iodine-125 seed strand for the treatment of hepatocellular carcinoma with portal vein tumour thrombosis versus TACE alone: a two-arm, randomised clinical trial. *J Cancer Res Clin Oncol*. 2014;140(2): 211-219.

21. Chen K, Xia Y, Wang H, Xiao F, Xiang G, Shen F. Adjuvant iodine-125 brachytherapy for hepatocellular carcinoma after complete hepatectomy: a randomized controlled trial. *PLoS One*. 2013;8(2):e57397.

22. Hui D, Qiang L, Jian W, Ti Z, Da-Lu K. A randomized, controlled trial of postoperative adjuvant cytokine-induced killer cells immunotherapy after radical resection of hepatocellular carcinoma. *Dig Liver Dis*. 2009;41(1):36-41.

23. Pan QZ, Wang QJ, Dan JQ, et al. A nomogram for predicting the benefit of adjuvant cytokine-induced killer cell immunotherapy in patients with hepatocellular carcinoma. *Sci Rep*. 2015;5:9202.

24. Liu L, Zhang W, Qi X, et al. Randomized study of autologous cytokine-induced killer cell immunotherapy in metastatic renal carcinoma. *Clin Cancer Res*. 2012;18(6):1751-1759.

25. Di Stasi A, Tey SK, Dotti G, et al. Inducible apoptosis as a safety switch for adoptive cell therapy. *N Engl J Med*. 2011;365(18): 1673-1683.

26. Lee JH, Lee JH, Lim YS, et al. Adjuvant immunotherapy with autologous cytokine-induced killer cells for hepatocellular carcinoma. *Gastroenterology*. 2015;148(7):1383-1391.e6.

27. Kuçi S, Rettinger E, Voss B, et al. Efficient lysis of rhabdomyosarcoma cells by cytokine-induced killer cells: implications for adoptive immunotherapy after allogeneic stem cell transplantation. *Haematologica*. 2010;95(9):1579-1586.

28. Zhang Q, Wang L, Luo C, et al. Phenotypic and functional characterization of cytokine-induced killer cells derived from preterm and term infant cord blood. *Oncol Rep*. 2014;32(5):2244-2252.

29. Nishimura R, Baker J, Beilhack A, et al. In vivo trafficking and survival of cytokine-induced killer cells resulting in minimal GVHD with retention of antitumor activity. *Blood*. 2008;112(6):2563-2574.

30. Fang L, Gong J, Wang Y, et al. MICA/B expression is inhibited by unfolded protein response and associated with poor prognosis in human hepatocellular carcinoma. *J Exp Clin Cancer Res*. 2014; 33:76.

31. Zhang J, Xu Z, Zhou X, et al. Loss of expression of MHC class I-related chain A (MICA) is a frequent event and predicts poor survival in patients with hepatocellular carcinoma. *Int J Clin Exp Pathol*. 2014;7(6):3123-3131.

32. Huang B, Sikorski R, Sampath P, Thorne SH. Modulation of NKG2D-ligand cell surface expression enhances immune cell therapy of cancer. *J Immunother*. 2011;34(3):289-296.

33. Guerra N, Tan YX, Joncker NT, et al. NKG2D-deficient mice are defective in tumor surveillance in models of spontaneous malignancy. *Immunity*. 2008;28(4):571-580.